

Comparison of shell model results of even-even Se isotopes

P.C. Srivastava

Department of Physics, Indian Institute of Technology, Roorkee - 247667, India

E-mail: pcsrifph@iitr.ernet.in

M. J. Ermamatov

Instituto de Ciencias Nucleares, Universidad Nacional Autónoma de México, 04510 México, D.F., Mexico

Institute of Nuclear Physics, Ulughbek, Tashkent 100214, Uzbekistan

Abstract.

Comprehensive set of shell model calculations for $^{78-84}\text{Se}$ isotopes have been performed with recently derived interactions, namely JUN45 and jj44b for $f_{5/2}pg_{9/2}$ space. To study the importance of the proton excitations across $Z = 28$ shell in this region mentioned by Cheal *et al.* [Phys. Rev. Lett. **104**, 252502 (2010)], calculation for $fp_{g_{9/2}}$ valence space using an $fp_{g_{9/2}}$ effective interaction with ^{48}Ca as core and imposing a truncation has also been performed. Comparison of the calculations with experimental data show that the predicted results of jj44b interaction are in good agreement with experimental data.

PACS numbers: 21.60.Cs, 27.50.+e

1. Introduction

The nuclei near $Z = 28$ region are subject of intensive research of both experimental and theoretical investigations [1, 2, 3]. In particular, the region of neutron-rich nuclei around $N = 40$ to $N = 50$ shows an evolution of shell structure. The nucleon-nucleon interaction, the spin-orbit, tensor part, and three-body effect play an important roles in the shell evolutions. Due to tensor interactions, the nuclear mean field undergoes variations with neutron excess. This leads to monopole migration, which is observed in both side of stability line. As we approach towards the neutron drip line, the neutron density becomes very diffused, which can also leads to shell quenching. Further motivations for nuclear structure studies are for understanding the other open questions like, how does the filling of neutron orbitals beyond $N = 28$ around ^{48}Ca influence the shell structure, what is the role of tensor part of proton-neutron interaction, how does the spin-orbit splitting between $f_{5/2}$ and $f_{7/2}$ evolve when approaching $N = 50$, and what is the specific role of particle-hole excitations through $Z = 28$ and $N = 40$ shell gaps for the onset of deformation below and above ^{78}Ni .

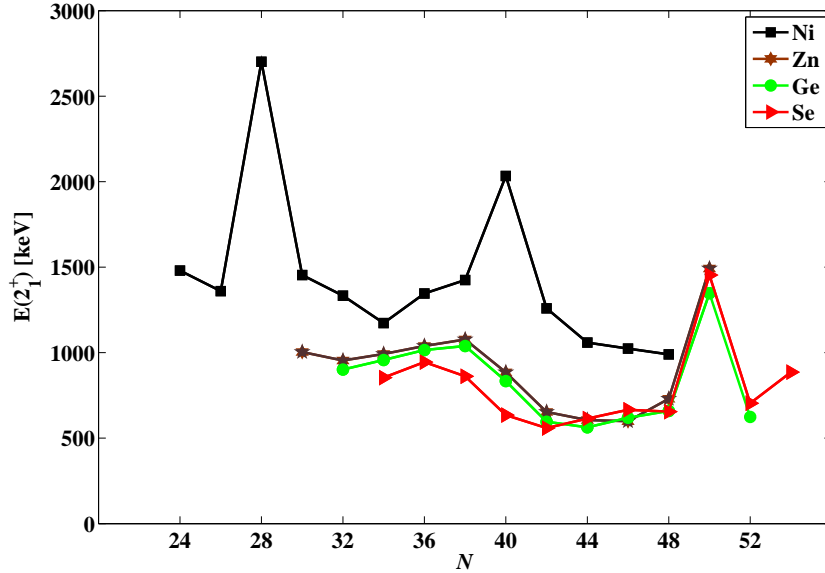


Figure 1. Systematic of the experimentally observed $E(2_1^+)$ for $Z = 28$ to $Z = 34$ near the $N = 28$, 40 and 50 shell closure.

To study the proton excitations across $Z = 28$ gap many experimental investigations have been performed for Cu [4], Ga [5] and As [6] isotopes. The inversion of $\pi f_{5/2}$ and $\pi p_{3/2}$ orbitals for Cu isotopes have been established while measuring magnetic moments for the ground-state. In case of $^{71-81}\text{Ga}$ isotopes experimental measurement of spin and moments reveal that there is structure change between $N = 40$ and $N = 50$. The $\pi f_{5/2}$ orbital dominant in the g.s. of ^{79}Ga and for ^{81}Ga , $5/2^-$ level become ground state. The evolution of structure can be seen from emptying of $\pi p_{3/2}$

orbital to $\pi f_{5/2}$ is started as we move from ^{71}Ga to ^{79}Ga . Finally $I^\pi=5/2^-$ become ground state for ^{81}Ga . In case of ^{79}Ga , the $f_{5/2}pg_{9/2}$ space fail to explain correctly the magnetic and electric quadrupole moment. Thus, it is crucial to include $\pi f_{7/2}$ orbital in the model space to study the effect of proton excitations across the $Z = 28$ effect. In case of As ($Z = 33$), recent experimental investigation by Astier et al [6] suggests that $f_{5/2}pg_{9/2}$ space is not enough to explain quadrupole excitation built on the $5/2_1^-$ and $9/2_1^+$ state of ^{81}As .

In this work, shell model calculation for $^{78-83}\text{Se}$ isotopes in two different model spaces $f_{5/2}pg_{9/2}$ and $fp_{g_{9/2}}$ have been performed. The aim of this study to study the importance of proton excitations across $Z = 28$ gap. One of us recently reported importance of $\pi f_{7/2}$ orbital for predicting moments of Ga isotopes [7]. In Fig. 1, the systematics of 2^+ for Ni to Se are shown. This figure shows the persistence of $N = 50$ shell closure while $N = 40$ disappears as we move from Ni to Se.

In section 2 the details about shell model calculations is described and then spectroscopic results for even-even $^{78,80,82,84}\text{Se}$ are presented in section 3. In section 4, transition probability, quadrupole moments and occupation numbers are presented. Finally section 5 gives the concluding remarks.

2. Details of model spaces and interactions

The present shell model calculations have been carried out in the $f_{5/2}pg_{9/2}$ and $fp_{g_{9/2}}$ spaces. In the $f_{5/2}pg_{9/2}$ valence space the calculations have been performed with the interactions JUN45 [8] and jj44b [9]. The single-particle energies for the $1p_{3/2}$, $0f_{5/2}$, $1p_{1/2}$ and $0g_{9/2}$ single-particle orbits employed in conjunction with the JUN45 interaction are -9.8280, -8.7087, -7.8388, and -6.2617 MeV respectively. In the case of the jj44b interaction they are -9.6566, -9.2859, -8.2695, and -5.8944 MeV, respectively. The core is ^{56}Ni , i.e. $N = Z = 28$, and the calculations are performed in this valence space without truncation.

In the $fp_{g_{9/2}}$ valence space, we use a ^{48}Ca core, i.e. only the protons are active in the $f_{7/2}$ orbital, and the interaction $fp_{g_{9/2}}$ reported by Sorlin et al [10]. The single-particle energies are 0.0, 2.0, 4.0, 6.5 and 9.0 MeV for the $0f_{7/2}$, $1p_{3/2}$, $1p_{1/2}$, $0f_{5/2}$, and $0g_{9/2}$ orbits, respectively. Since the dimensionality of this valence space is prohibitively large, we have introduced a truncation by allowing t_π particle-hole excitations from the $\pi f_{7/2}$ orbital to the upper fp orbitals ($p_{3/2}$, $f_{5/2}$, $p_{1/2}$) for protons and t_ν particle-hole excitations from the upper fp orbitals to the $\nu g_{9/2}$ orbital for neutrons. The maximum allowed value for t_π and t_ν is four. The maximal dimension 165000813 ($\sim 10^8$) is reached for positive parity in the case of ^{78}Se when using $f_{5/2}pg_{9/2}$ space with ^{56}Ni core since neutron number is furthest from the closed shell for this nucleus among the Se isotopes considered in this work. In case of ^{78}Se computing time ~ 21 days for both parity. The calculations were performed with shell-model code ANTOINE [11].

3. Spectra analysis

The results for the three interactions for different model spaces used in the calculations are presented with respect to the experiment in Figs.2-5. Earlier shell model result in 28-50 model space for pairing plus quadrupole-quadrupole interaction has been reported in literature by Yoshinaga *et al.* [12]. Further this work will add more information to the earlier work [12], by including $f_{7/2}$ orbital in the model space to study the proton excitation across $Z = 28$ shell. The shell model structure of Se isotopes was discussed in [8] using JUN45 interaction. The results for the three interactions used in the calculations are presented with respect to the experiment.

3.1. ^{78}Se

Comparison of the calculated values of the energy levels of ^{78}Se with the experimental data is shown in Fig. 2. All the three interactions correctly reproduces the experimental sequence of 0_1^+ , 2_1^+ , 4_1^+ , 6_1^+ , 8_1^+ , 10_1^+ and 12_1^+ levels at 614, 1503, 2546, 3585, 4625 and 8784 keV, respectively. In case of JUN45, the calculated 2_1^+ , 4_1^+ and 6_1^+ levels are 134, 240 and 251 keV higher than the experimental ones, while remained 8_1^+ , 10_1^+ and 12_1^+ are predicted 117, 323 and 397 keV lower than experimental levels. The 2_1^+ level calculated by jj44b is only 60 keV higher as compared to its experimental counterpart. Difference between experimental and calculated energies is increased by increasing the excited energies reaching 433 keV at 12_1^+ . All the levels calculated by fpg interaction is much lower than in the experiment. By the increasing spin the difference between the calculated and experimental levels is increased and it become rather 1751 keV when reaching 12_1^+ level.

In all the calculations first two 0^+ and 2^+ levels of the second positive-parity band are interchanged with respect to experimental ones. The next 0^+ and 3^+ levels are located higher than in the experiment in all calculations. The experimental sequence levels 2^+ , 4^+ , 4^+ and 5^+ at 1996, 2191, 2682 and 2735 keV are better reproduced by the JUN45 calculation. The two 6^+ levels appear in all calculations after the 5^+ level which have not been observed in the experiment. The last three levels of this band calculated by the JUN45 interaction excellently agree with the experimental data. Experimental levels of this band measured up to 10^+ and many odd spin levels 1^+ , 7^+ , 9^+ , which appear in the calculations, have not been observed in the experiment.

The experimental negative-parity levels start with the 3^- level. The first negative-parity level is 4^- in both JUN45 and jj44b calculations, while it is 2^- in the fpg calculation. In the JUN45 calculation the first few levels are much compressed than in the experiment. The spins and parities of (7^-) , (8^-) , (9^-) , and (9^-) levels which is not confirmed in the experiment, are predicted by all calculations as negative parity levels. The sequence of experimentally observed levels starting from 1^- is exactly the same as in the jj44b calculation.

3.2. ^{80}Se

In Fig. 3 we have shown the comparison of the values of the energy levels calculated by JUN45, jj44b and *fpg* interactions with experimental data. The values calculated by JUN45 are in very good agreement with the all levels of the first experimental positive-parity band which are available up to 10^+ . The jj44b calculation predicts higher values after 4^+ , while the values predicted by the *fpg* calculation are lower up to 4^+ and then the 6^+ level is higher. The 8^+ and 10^+ levels are again lower than in the experiment.

The first two levels of the second positive-parity band are interchanged with respect to those of ^{78}Se in jj44b calculation. The sequence of these levels are not changed with respect to those of ^{78}Se in JUN45 calculation. In the *fpg* calculation 2^+ level is lowest in the second positive-parity band. The 4^+ level is predicted much lower than in the experiment, while the second 0^+ and 2^+ levels are higher in this band than in the experiment. The second 4^+ level is only 17 keV higher than in the experiment. Then three 6^+ levels in succession come in the calculation. The 8^+ in the calculation is much higher than in the experiment. For odd spin-positive-parities, which we have shown in the third column, all the calculation predict two levels for each spin (1^+ and 1^+ , 3^+ and 3^+ , ..). In the experiment only one 1^+ and 3^+ are measured, first of which is higher than all 1^+ levels in all calculation, while second of them lower than 3_1^+ level in all calculations.

The lowest negative-parity level according to JUN45 and jj44b calculations are 1^- , which is much higher in the experiment, however the second and the third 1^- levels are closer to the experimental ones in both calculations. Four 3^- levels are measured in the experiment. For both JUN45 and jj44b calculations the reported three 3^- levels are located approximately the same in both calculations. We have also reported three 5^- levels in all calculations. All of them are lower than experimentally measured two 5^- levels.

3.3. ^{82}Se

As is seen from Figure 4 in all calculated levels in the first column are in similar pattern to experimental one. Better values are predicted by JUN45 calculation.

In all calculations the first level in the second column is 0^+ level like in the experiment. Closest value of this level is predicted by JUN45. The spacing between the first and the second 2^+ levels in the second column are less than that of in the experiment in all calculations. In JUN45 calculation first of two 4^+ levels is located lower while the second one is higher than in the experiment. In jj44b calculation both of them are much higher than in the experiment. In *fpg* calculation the first 4^+ is only 8 keV higher than in the experiment. The second 0^+ is predicted well by jj44b calculation.

Among the positive-parity odd spin levels only 9^+ and (11) level energies measured in the experiment. The (11) level's parity is predicted to be positive by the calculations. As in the case of previous isotopes there are many other 1^+ , 3^+ , 5^+ levels in the calculation which are not measured in the experiment.

As is seen from the Figure 4 agreement of the all calculated values of negative-parity levels with the experimental data is improved very much as compared to the $^{78,80}\text{Se}$ isotopes.

3.4. ^{84}Se

The levels of the first column of Figure 5 are predicted better by jj44b calculation. Also 6^+ level is little bit higher than the in JUN45, spacings between the levels very much like to the experimental ones.

In all calculations the first positive-parity level in the second column is 0^+ as in the experiment. The sequences of 0_1^+ , 0_2^+ and 2_1^+ , 2_2^+ levels is the same with the experimental one in jj44b calculation and spacings between them are larger than in the experiment. Sequence of the pair of these levels are different from the experimental one in JUN45 and *fpg* calculations and spacing between them are much larger than in the experiment. The 4_1^+ , and 4_2^+ levels are located much lower than in the experiment in all calculations.

The 1^+ and 3^+ levels appearing in the calculations have not been measured in the experiment. The measured 5^+ level is predicted better by JUN45. The 7^+ level is located very high in all the calculations as compared to experimental one.

The structure of the negative-parity levels for ^{84}Se is changed so drastically as compared to previous isotopes and both JUN45 and jj44b calculations fail to explain it.

4. Transition probability, quadrupole moments and occupation numbers analysis

4.1. *E2 transition probability and quadrupole moments*

The calculated $B(E2)$ transitions are shown in table 1. In case of $^{78,80}\text{Se}$, the results predicted by *fpg* interaction show better agreement with experimental data. While for $^{82,84}\text{Se}$, the jj44b interaction results are more reasonable. Thus we may conclude that proton excitation across $Z = 28$ shell for lighter Se isotopes are important. We have also calculated static quadrupole moments as shown in table 2. For the first 2^+ state, the JUN45 and jj44b interaction correctly predict sign of quadrupole moments for $^{78,80,82}\text{Se}$. The *fpg* interaction predicts positive sign for ^{78}Se . The overall agreement for quadrupole moments predicted by jj44b is better.

4.2. *Occupation numbers*

In Fig. 6, we show the proton/neutron occupation numbers of *fpg*-shell orbits for 0_1^+ and 2_1^+ levels. The proton occupancies increasing smoothly in the $f_{5/2}$ orbital, while $p_{3/2}$ decreasing. But beyond $N = 46$, in case of JUN45 interaction the change in occupancy of these two orbitals are very significant. With both interaction the occupancy of proton $p_{1/2}$ and $g_{9/2}$ orbitals are similar. As the neutron number increases the occupation

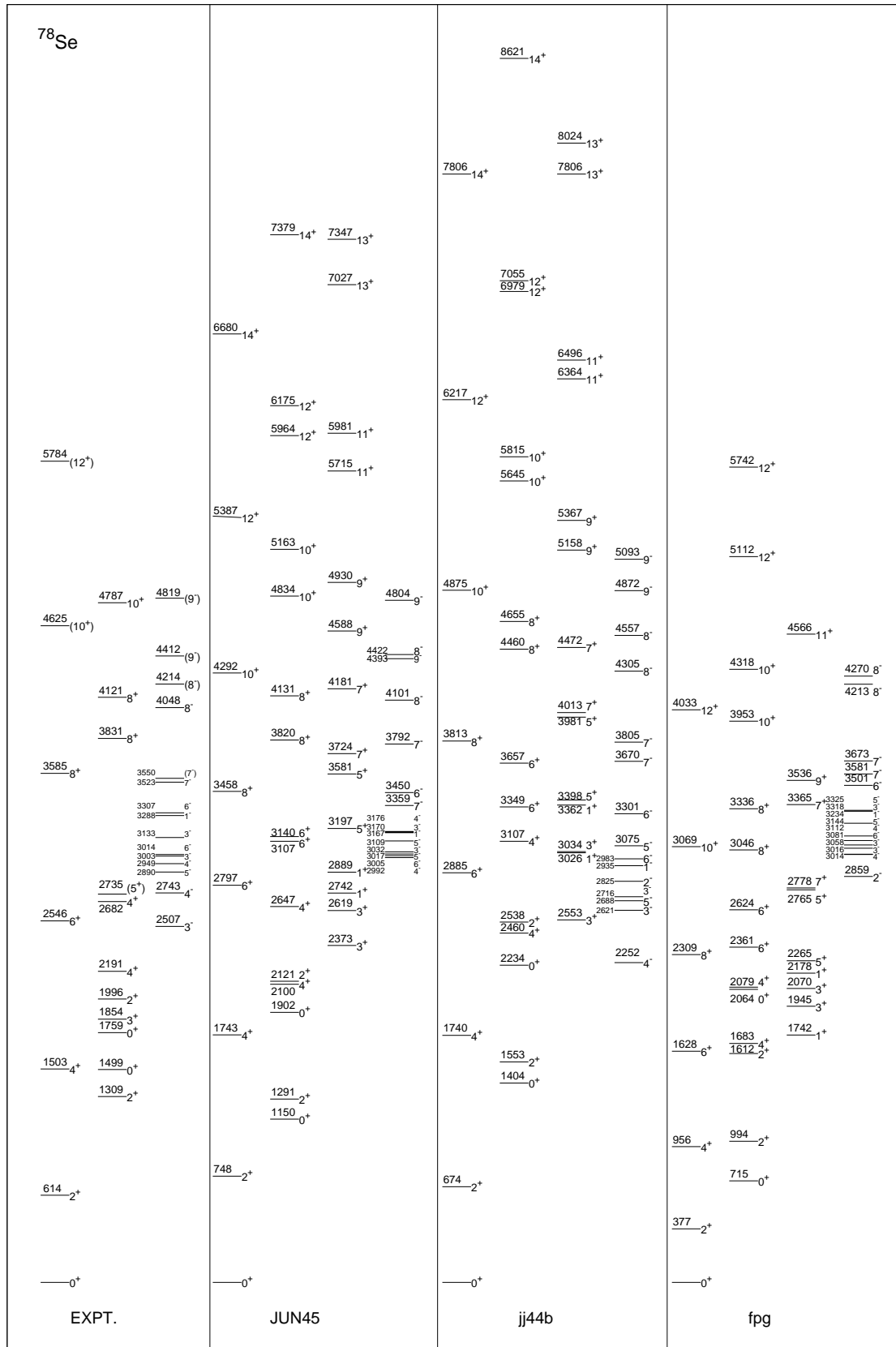


Figure 2. Comparison of experimental and calculated excitation spectra of ^{78}Se with three different interactions.

⁸⁰ Se			
<p>4673 (10⁺)</p> <p>4464 (1⁻) 4436 (5⁻)</p> <p>4130 (3⁻) 3996 (5⁻) 3976 3870 (1⁻) 3814 (8⁺) 3754 (3⁻)</p> <p>3635 (8⁺)</p> <p>3350 (1⁺) 3284 (3⁻)</p> <p>3036 6⁺ 3033 4⁺</p> <p>2895 6⁺</p> <p>2826 (6⁺)</p> <p>2717 3⁻</p> <p>2495 (4⁺)</p> <p>2121 (3⁺) 1960 2⁺ 1873 (0⁺)</p> <p>1701 4⁺</p> <p>1479 0⁺ 1449 2⁺</p> <p>666 2⁺</p> <p>— 0⁺</p> <p>EXPT.</p>	<p>7716 14⁺</p> <p>7542 13⁺</p> <p>6951 14⁺</p> <p>7003 13⁺</p> <p>6391 12⁺</p> <p>6098 12⁺</p> <p>6119 11⁺</p> <p>5893 11⁺</p> <p>5793 12⁺</p> <p>5397 10⁺</p> <p>5244 9⁺</p> <p>5058 10⁺</p> <p>4832 9⁺</p> <p>4638 10⁺</p> <p>4499 8⁺</p> <p>4210 8⁺</p> <p>4422 1⁻</p> <p>4196 1⁻</p> <p>4154 7⁻</p> <p>3809 7⁺</p> <p>3671 5⁺</p> <p>3652 5⁺</p> <p>3463 5⁻ 3368 3⁻</p> <p>3264 6⁺</p> <p>3099 1⁺</p> <p>3054 3⁻ 2963 5⁻ 2860 3⁻ 2756 1⁻</p> <p>2888 6⁺</p> <p>2878 4⁺</p> <p>2874 1⁺</p> <p>2491 2⁺</p> <p>2582 3⁺</p> <p>2486 4⁺</p> <p>2392 3⁺</p> <p>2128 0⁺</p> <p>1784 4⁺</p> <p>1716 2⁺</p> <p>1514 0⁺</p> <p>726 2⁺</p> <p>— 0⁺</p> <p>JUN45</p>	<p>8717 14⁺</p> <p>8327 14⁺</p> <p>8363 13⁺</p> <p>7862 13⁺</p> <p>7510 12⁺</p> <p>7120 12⁺</p> <p>6854 12⁺</p> <p>6542 11⁺</p> <p>6253 11⁺</p> <p>6144 10⁺ 6087 10⁺</p> <p>5809 9⁺</p> <p>5695 9⁺</p> <p>5492 10⁺</p> <p>5352 8⁺</p> <p>5372 7⁺</p> <p>4966 8⁺</p> <p>4758 7⁺</p> <p>4304 8⁺</p> <p>4252 5⁺</p> <p>4194 1⁻ 4193 7⁻</p> <p>4080 6⁺ 3947 6⁺</p> <p>3773 5⁺</p> <p>3688 5⁻</p> <p>3560 6⁺</p> <p>3262 4⁺</p> <p>3391 1⁺</p> <p>3473 5⁻ 3410 5⁻ 3329 7⁻</p> <p>3207 5⁻ 3135 3⁻</p> <p>3055 1⁺</p> <p>3016 3⁺</p> <p>2896 4⁺</p> <p>2508 2⁺</p> <p>2362 0⁺</p> <p>2393 3⁺</p> <p>1961 4⁺</p> <p>1959 0⁺ 1799 2⁺</p> <p>696 2⁺</p> <p>— 0⁺</p> <p>jj44b</p>	<p>7467 13⁺</p> <p>7092 14⁺</p> <p>6493 14⁺</p> <p>6563 12⁺</p> <p>6433 13⁺</p> <p>6349 12⁺</p> <p>6031 11⁺</p> <p>5454 10⁺</p> <p>5233 12⁺</p> <p>5238 11⁺</p> <p>5056 9⁺</p> <p>4918 10⁺</p> <p>4849 9⁺</p> <p>4601 7⁺</p> <p>4465 8⁺</p> <p>4439 7⁺</p> <p>4305 10⁺</p> <p>4188 8⁺</p> <p>3886 3⁻ 3798 7⁻</p> <p>3748 5⁻</p> <p>3559 8⁺</p> <p>3704 6⁺</p> <p>3512 5⁺</p> <p>3422 6⁺</p> <p>3139 5⁺</p> <p>3244 3⁻ 3220 1⁻</p> <p>3011 6⁺</p> <p>2782 1⁺</p> <p>2665 3⁻ 2633 5⁻</p> <p>2512 4⁺</p> <p>2439 1⁺</p> <p>2305 0⁺</p> <p>2359 3⁺</p> <p>2141 2⁺</p> <p>1815 3⁺</p> <p>1750 0⁺ 1690 4⁺</p> <p>1690 4⁺</p> <p>1279 2⁺</p> <p>605 2⁺</p> <p>— 0⁺</p> <p>fpg</p>

Figure 3. Comparison of experimental and calculated excitation spectra of ⁸⁰Se with three different interactions.

^{82}Se	$\frac{8811}{14^+}$	$\frac{8908}{13^+}$ $\frac{8786}{13^+}$	
		$\frac{8195}{14^+}$	$\frac{8143}{13^+}$
	$\frac{7869}{13^+}$	$\frac{7842}{12^+}$	$\frac{7683}{14^+}$ $\frac{7683}{13^+}$
	$\frac{7559}{13^+}$	$\frac{7414}{12^+}$	$\frac{7360}{12^+}$
	$\frac{7075}{14^+}$	$\frac{7235}{14^+}$ $\frac{7194}{12^+}$	
	$\frac{6863}{12^+}$	$\frac{6851}{12^+}$	
	$\frac{6613}{12^+}$	$\frac{6684}{10^+}$ $\frac{6715}{11^+}$	$\frac{6614}{11^+}$
	$\frac{6339}{11^+}$	$\frac{6231}{10^+}$ $\frac{6318}{9^+}$	$\frac{6247}{10^+}$
$\frac{6129}{(12)}$		$\frac{6008}{11^+}$	$\frac{6149}{12^+}$ $\frac{6008}{10^+}$ $\frac{5975}{9^+}$
	$\frac{5794}{12^+}$ $\frac{5842}{10^+}$	$\frac{5881}{10^+}$	
$\frac{5687}{(11)}$	$\frac{5650}{10^+}$ $\frac{5542}{9^+}$	$\frac{5590}{8^+}$ $\frac{5656}{7^+}$	$\frac{5659}{11^+}$
$\frac{5457}{(10^+)}$	$\frac{5200}{10^+}$ $\frac{5177}{11^+}$	$\frac{5241}{8^+}$ $\frac{5242}{9^+}$	$\frac{5492}{10^+}$ $\frac{5389}{8^+}$ $\frac{5229}{7^+}$
	$\frac{4983}{(9^+)}$ $\frac{5029}{(1^+)}$	$\frac{5001}{1^-}$	$\frac{5042}{7^+}$
	$\frac{4809}{(1^+)}$ $\frac{4854}{8^+}$	$\frac{4702}{6^+}$	$\frac{4902}{8^+}$ $\frac{4995}{9^+}$
	$\frac{4700}{9^+}$ $\frac{4584}{1^-}$	$\frac{4509}{6^+}$ $\frac{4506}{5^+}$	
	$\frac{4509}{8^+}$ $\frac{4352}{1^-}$	$\frac{4218}{5^+}$ $\frac{4205}{1^-}$	$\frac{4129}{6^+}$ $\frac{4090}{5^+}$ $\frac{4138}{1^-}$
	$\frac{4016}{5^+}$	$\frac{3819}{8^+}$ $\frac{3745}{5^-}$	$\frac{3940}{6^+}$ $\frac{3866}{5^+}$ $\frac{3973}{1^-}$
	$\frac{3896}{6^+}$ $\frac{3837}{6^+}$	$\frac{3633}{6^+}$ $\frac{3604}{4^+}$	$\frac{3642}{3^-}$ $\frac{3634}{7^-}$
	$\frac{3794}{(7)}$ $\frac{3649}{5^+}$	$\frac{3509}{3^-}$ $\frac{3382}{7^-}$	$\frac{3474}{3^+}$ $\frac{3238}{5^-}$
$\frac{3518}{8^+}$ $\frac{3591}{2^+}$ $\frac{3466}{0^+}$	$\frac{3468}{8^+}$ $\frac{3261}{4^+}$	$\frac{3288}{1^+}$ $\frac{3224}{3^+}$ $\frac{3266}{3^-}$	$\frac{3163}{1^+}$ $\frac{3076}{3^-}$
$\frac{3454}{(5)}$ $\frac{3378}{(3)}$	$\frac{3216}{6^+}$ $\frac{3201}{1^+}$ $\frac{3108}{3^+}$	$\frac{3200}{4^+}$ $\frac{3098}{2^+}$ $\frac{3111}{1^+}$ $\frac{2969}{3^+}$ $\frac{3006}{5^-}$	$\frac{3389}{6^+}$ $\frac{3381}{4^+}$ $\frac{2891}{0^+}$
$\frac{3145}{6^+}$ $\frac{3103}{(4^+)}$ $\frac{3009}{3^-}$ $\frac{2894}{5^-}$	$\frac{2783}{0^+}$ $\frac{2863}{1^+}$	$\frac{2607}{2^+}$ $\frac{2603}{0^+}$	$\frac{2597}{2^+}$ $\frac{2558}{4^+}$
$\frac{2626}{(0^+)}$ $\frac{2550}{4^+}$	$\frac{2449}{2^+}$ $\frac{2392}{4^+}$ $\frac{2289}{3^+}$	$\frac{2111}{0^+}$	$\frac{2311}{3^+}$ $\frac{2295}{5^-}$
	$\frac{2087}{2^+}$	$\frac{2002}{4^+}$	$\frac{1952}{4^+}$
	$\frac{1848}{4^+}$		$\frac{1538}{2^+}$
$\frac{1735}{4^+}$ $\frac{1731}{2^+}$	$\frac{1397}{0^+}$	$\frac{719}{2^+}$	$\frac{782}{2^+}$ $\frac{706}{0^+}$
$\frac{1410}{0^+}$			
$\frac{655}{2^+}$	$\frac{729}{2^+}$		
$\frac{0^+}{0^+}$	$\frac{0^+}{0^+}$	$\frac{0^+}{0^+}$	$\frac{0^+}{0^+}$
EXPT.	JUN45	jj44b	fpg

Figure 4. Comparison of experimental [13] and calculated excitation spectra of ^{82}Se with three different interactions.

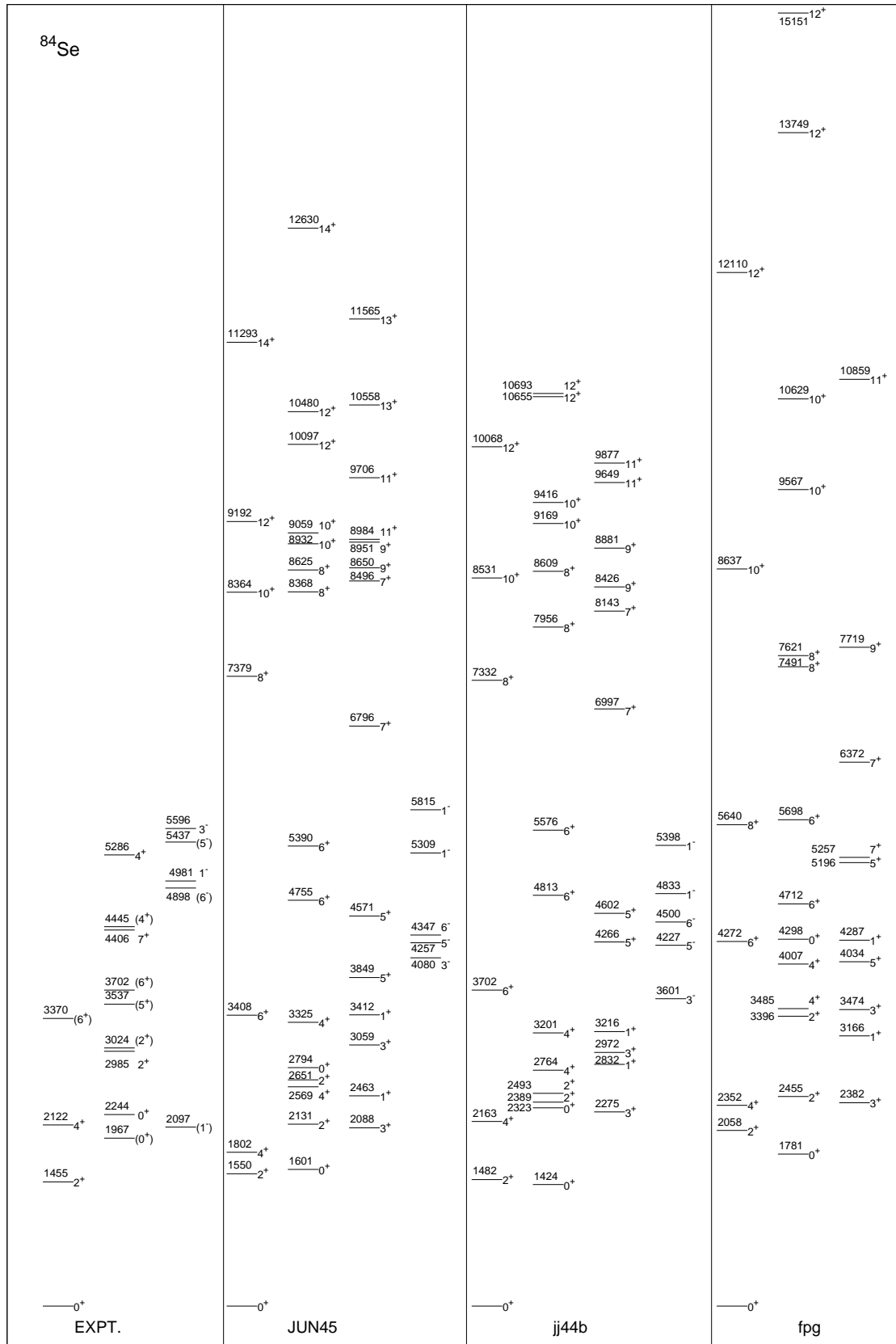


Figure 5. Comparison of experimental [14, 15, 16] and calculated excitation spectra of ^{84}Se with three different interactions.

Table 1. $B(E2)$ reduced transition strength in W.u. Effective charges $e_p = 1.5$ $e_n = 0.5$ were used. Experimental values were taken from the NNDC database.

	^{78}Se	^{80}Se	^{82}Se	^{84}Se
$\text{BE}(2_1^+ \rightarrow 0_1^+)$				
Experiment	32.8(4.5)	24.2 (0.4)	16.7 (0.3)	N/A
JUN45	18.83	16.53	13.88	6.64
jj44b	20.74	18.88	15.33	8.37
fpg	30.87	24.08	16.33	8.22
$\text{BE}(4_1^+ \rightarrow 2_1^+)$				
Experiment	$38.2^{+5.6}_{-5.1}$	34.7 (1.1)	18.7 (3.0)	N/A
JUN45	25.47	21.40	19.60	1.96
jj44b	27.23	25.65	20.77	0.005
fpg	46.27	32.85	25.86	1.42
$\text{BE}(6_1^+ \rightarrow 4_1^+)$				
Experiment	48(14)	N/A	N/A	N/A
JUN45	23.69	16.81	15.42	1.02
jj44b	24.22	21.92	18.01	3.25
fpg	48.92	32.01	24.42	0.12
$\text{BE}(8_1^+ \rightarrow 6_1^+)$				
Experiment	57(19)	N/A	0.56 (0.03)	N/A
JUN45	13.01	7.45	0.38	0.0008
jj44b	21.86	1.27	0.31	0.002
fpg	49.01	7.13	0.57	1.13

number of $\nu g_{9/2}$ orbital increases drastically. The neutron number occupation show a similar distribution for 2_1^+ as in the ground state.

Table 2. Electric quadrupole moments, Q_s (in eb), with the three different interactions (the effective charges $e_p=1.5$, $e_n=0.5$ are used in the calculation).

	^{78}Se	^{80}Se	^{82}Se	^{84}Se
$Q(2_1^+)$				
Experiment	-0.20 (7)	-0.31 (7)	-0.22 (7)	N/A
JUN45	-0.13	-0.31	-0.33	+0.01
jj44b	-0.32	-0.36	-0.37	-0.27
fpg	+0.47	-0.35	-0.36	+0.04
$Q(2_2^+)$				
Experiment	+0.17 (9)	N/A	N/A	N/A
JUN45	+0.13	+0.28	+0.24	-0.09
jj44b	+0.30	+0.35	+0.27	+0.13
fpg	-0.33	+0.36	+0.28	+0.007
$Q(4_1^+)$				
Experiment	-0.68 (15)	N/A	N/A	N/A
JUN45	-0.09	-0.35	-0.39	+0.10
jj44b	-0.36	-0.40	-0.42	+0.18
fpg	+0.63	-0.29	-0.43	+0.15

5. Summary

In summary, comprehensive study for the structure of neutron-rich even-even Se isotopes have been carried out using large-scale shell-model calculations for two spaces: full $f_{5/2}pg_{9/2}$ space and $fpg_{9/2}$ space with ^{48}Ca core.

The following broad conclusions can be drawn:

- The overall calculated results for the energy levels, $B(E2)$ s and quadrupole moments are in good agreement with the experimental data.
- The $E2$ transitions, quadrupole moments analysis show the importance of proton excitations across $Z = 28$ shell for $fpg_{9/2}$ space.
- For $^{78-80}\text{Se}$ the $B(E2)$ values predicted by fpg transitions are in better agreement with experimental data.
- The result (wave functions) of ^{82}Se , may be used for calculating nuclear transition matrix elements and finally half-live for this nucleus which is a good candidate for neutrinoless double beta decay.
- It is also important while tuning the effective interaction we can also take

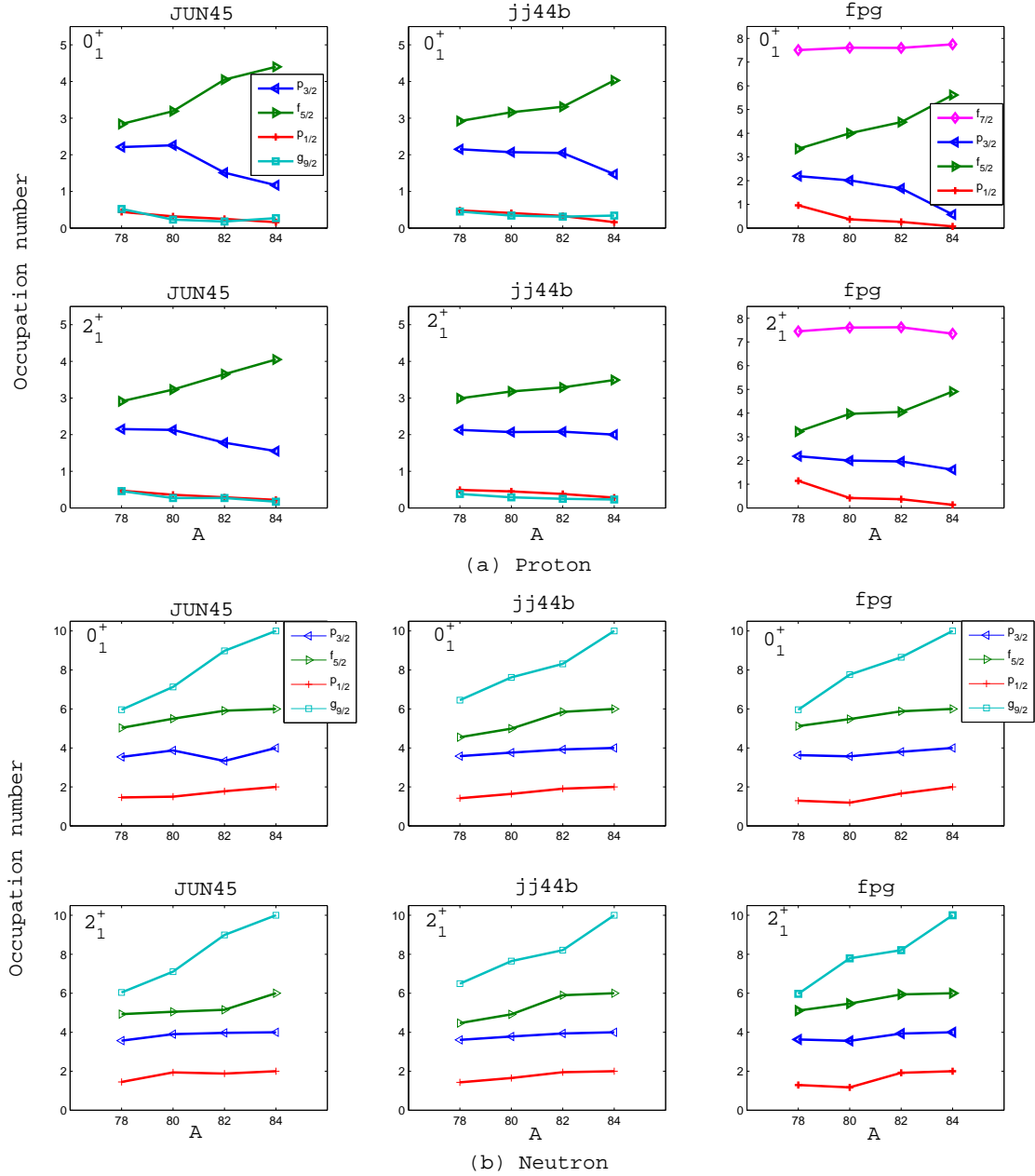


Figure 6. (Color online) Proton/Neutron occupation numbers of the JUN45 and jj44b ($p_{3/2}$, $f_{5/2}$, $p_{1/2}$ and $g_{9/2}$ -shell orbits) and *fpg* ($f_{7/2}$, $p_{3/2}$, $f_{5/2}$, $p_{1/2}$ -shell orbits) interactions- for two low-lying states in even-even Se isotopes. (Upper panel) 0_1^+ states; (lower panel) 2_1^+ states.

experimentally known quadrupole moment as a parameter to increase predictive power of effective interaction.

- Further theoretical development is needed by enlarging model space by including $\nu d_{5/2}$ orbital to study simultaneously proton and neutron excitations across $Z = 28$ and $Z = 50$ shell, respectively.

Acknowledgments

Thanks are due to E. Padilla- Rodal for useful discussions during this work. All the shell-model calculations have been performed at KanBalam computational facility of DGCTIC-UNAM, Mexico. MJE acknowledges support from grant No. 17901 of CONACyT projects CB2010/155633 and F2-FA-F177 of Uzbekistan Academy of Sciences.

References

- [1] Padilla-Rodal E *et al* 2005 Phys. Rev. Lett. **94** 122501
- [2] Heyde K 2013 Phys. Scr. **T152** 014006
- [3] Otsuka T 2013 Phys. Scr. **T152** 014007
- [4] Flanagan K T *et al* 2009 Phys. Rev. Lett. **103** 142501
- [5] Cheal B *et al* 2010 Phys. Rev. Lett. **104** 252502
- [6] Porquet M -G *et al* 2011 Phys. Rev. C **84** 054305
- [7] Srivastava P C 2012 J. Phys. G **39** 015102
- [8] Honma M, Otsuka T, Mizusaki T and Hjorth-Jensen M 2009 Phys. Rev. C **80** 064323
- [9] B.A. Brown and A.F. Lisetskiy (unpublished).
- [10] Sorlin O *et al* 2002 Phys. Rev. Lett. **88** 092501
- [11] Caurier E, Martínez-Pinedo G, Nowacki F, Poves A, and Zuker A P 2005 Rev. Mod. Phys. **77** 427
- [12] Yoshinaga N, Higashiyama K, and Regan P H, Phys. Rev. C **78** 044320
- [13] Porquet M -G *et al* 2009 Eur. Phys. J. A. **39** 295
- [14] Gade A *et al* 2010 Phys. Rev. C **81** 064326
- [15] Prévost A *et al* 2004 Eur. Phys. J. A. **22** 391
- [16] Jones E F *et al* 2006 Phys. Rev. C **73** 017301